fibrotic liver tissue of humans and mice [10]. Thus, it has been speculated that the change in the expression of miR-29 is closely related to the development of liver fibrosis. Although analyses of miR-29 functions were performed on ECM metabolism in these reports, the cells used in these experiments were immortalized cell lines that had already been activated and had become myofibroblastic, which does not always reflect miR-29 function in quiescent HSCs *in vivo*. Therefore, it is important to evaluate the effect of miR-29 on the activation of primary-cultured HSCs. These cells are known to undergo spontaneous activation and transdifferentiation into myofibroblastic cells in culture, similarly to those *in vivo*. Activated HSCs express α-SMA and produce fibrogenic mediators, such as type I collagen and transforming growth factor-β (TGF-β).

Here, we show the effects of miR-29b on the activation of HSCs using freshly isolated primary-cultured mouse HSCs. Overexpression of miR-29b suppressed cell viability and the expression of α-SMA. These effects seemed to be independent of the activation of focal adhesion kinase (FAK), extracellular signal-regulated kinase (ERK), and phosphatidylinositol-3 kinase (PI3K)–Akt, but were partially dependent on the reduction of c-fos mRNA.

2. Materials and methods

2.1. Cells

Primary HSCs were isolated from 12- to 16-week-old male C57BL/6N mice (Japan SLC Inc., Shizuoka, Japan) by pronase–collagenase digestion and subsequent purification by a single-step Nycodenz gradient, as previously described [11]. All animals received humane care, and the experimental protocol was approved by the Committee of Laboratory Animals according to institutional guidelines. Isolated HSCs were cultured on plastic dishes or glass chamber slides in Dulbecco's modified Eagle's medium (DMEM) (Sigma Chemical Co., St. Louis, MO, USA) supplemented with 10% fetal bovine serum (FBS) (Invitrogen, Carlsbad, CA, USA), 100 U/ml penicillin, and 100 μg/ml streptomycin. The purity of cultures was evaluated by observation of the characteristic stellate cell shape using phase-contrast microscopy.

The human HSC line LX-2 was donated by Dr. Scott L. Friedman (Mount Sinai School of Medicine, New York, NY, USA) [12]. LX-2 cells were maintained in DMEM as described above.

2.2. Transient transfection of a miR-29b precursor

The miR-29b precursor (Ambion, Austin, TX, USA), which was a double-strand RNA mimicking the endogenous miR-29b precursor, and a negative control (Ambion) were transfected into mouse HSCs and LX-2 cells using Lipofectamine RNAiMAX (Invitrogen) at a final concentration of 10 nM in accordance with the manufacturer's instructions. Briefly, the miRNA precursor and Lipofectamine RNAiMAX were mixed at a ratio of 5 (pmol):1 (μl) in Opti-MEM I Reduced Medium (Invitrogen), incubated for 20 min at room temperature, and then added to the cultures.

2.3. Quantitative real-time PCR

Total RNA was extracted from cells using the miRNeasy Mini Kit (Qiagen, Valencia, CA, USA). Fifty nanograms of total RNA was reverse-transcribed to cDNA using the ReverTra Ace qPCR RT Kit (Toyobo, Osaka, Japan) in accordance with the manufacturer's instructions. Gene expression was measured by real-time PCR using cDNA, SYBR Green real-time PCR Master Mix (Toyobo), and a set of gene-specific oligonucleotide primers [alpha 1 (I) collagen (Col1a1): forward 5′-CCTGGCAAAGACGGACTCAAC-3′, reverse 5′-GCTGAAGT CATAACCGCCACTG-3′; alpha 2 (I) collagen (Col1a2): forward 5′-AA GGGTCCCTCTGGAGAACC-3′, reverse 5′-TCTAGAGCCAGGGAG AC-CCA-3′; α-SMA: forward 5′-TCCCTGGAGAAGAGCTACGAACT-3′, reverse 5′-AAGCGTTCGTTTCCAATGGT-3′; discoidin domain receptor (DDR) 2: forward 5′-CGAAAGCTTCCAGAGTTTGC-3′, reverse 5′-GCT TCACAACACCACTGCAC-3′; fibronectin (FN) 1: forward 5′-GATGCC GATCAGAAGTTTGG-3′, reverse 5′-GGTTGTGCAGATCTCCTCGT-3′; β1 integrin (ITGB1): forward 5′-CAACCACAACAGCTGCTTCTAA-3′, reverse 5′-TCAGCCCTCTTGAATTTTAATGT-3′; platelet-derived growth factor receptor-β (PDGFR-β): forward 5′-GCGTATCTATATCT TTGTGCCAGA-3′, reverse 5′-ACAGGTCCTCGGAG TCCAT-3′; c-fos: forward 5′-AGAAGGGGCAAAGTAGAGCA-3′, reverse 5′-CAGCTCC CTCCTCCGATT-3′; c-jun: forward 5′-CCAGAAGATGGTGTGGTGTTT-3′, reverse 5′-CTGACCCTCTCCCCTTGC-3′; glyceraldehyde-3-phosphate dehydrogenase (GAPDH): forward 5′-TGCACCACCAACTGCT-TAG-3′, reverse 5′-GGATGCAGGGATGATGTTC-3′] using an Applied Biosystems Prism 7500 (Applied Biosystems, Foster City, CA, USA). To detect miR-29b expression, the reverse transcription reaction was performed using a TaqMan microRNA Assay (Applied Biosystems) in accordance with the manufacturer's instructions. The expression level of GAPDH was used to normalize the relative abundance of mRNAs and miR-29b.

2.4. Immunoblots

Cells were lysed in RIPA buffer [50 mM Tris/HCl, pH7.5, 150 mM NaCl, 1% NP-40, 0.5% sodium deoxycholate, 0.1% sodium dodecyl sulfate (SDS)] containing Protease Inhibitor Cocktail, Phosphatase Inhibitor Cocktail 1, and Phosphatase Inhibitor Cocktail 2 (Sigma). Proteins (2.5–10 μg) were electrophoresed in a 5–20% gradient SDS–polyacrylamide gel (ATTO Co., Tokyo, Japan) and were then transferred onto Immobilon P membranes (Millipore, Bedford, MA, USA). After blocking, the membranes were incubated with primary antibodies [mouse monoclonal antibody against α-SMA (Dako, Ely, UK); rabbit polyclonal antibody against type I collagen (Rockland Immunochemicals, Inc., Gilbertsville, PA, USA); rabbit polyclonal antibodies against PDGFR-β and GAPDH (Santa Cruz Biotechnology Inc., Santa Cruz, CA, USA); rabbit polyclonal antibodies against FAK and phospho-FAK (Y397) (Cell Signaling Technology Inc., Beverly, MA, USA); and mouse monoclonal antibodies against ERK, phospho-ERK (T202/Y204), Akt, and phospho-Akt (S473) (Cell Signaling Technology Inc.)] followed by peroxidase-conjugated secondary antibodies (Dako). Immunoreactive bands were visualized by the enhanced chemiluminescence system (Amersham, Roosdaal, Netherlands) using a Fujifilm Image Reader LAS-3000 (Fuji Medical Systems, Stamford, CT, USA).

2.5. F-actin staining

HSCs on glass chamber slides were fixed in 4% paraformaldehyde in phosphate buffered saline (PBS) for 30 min and were permeabilized with 0.1% Triton X-100 in PBS for 5 min at room temperature. The nonspecific background signal was blocked with 1% bovine serum albumin (BSA) in PBS for 20 min. F-actin was stained with MFP488-phalloidin (Mobitec, Goettingen, Germany) in PBS with 1% BSA for 20 min. 4′,6-diamidino-2-phenylindole (DAPI) (Dojindo Laboratories, Kumamoto, Japan) was used for counterstaining.

2.6. Cell viability assay

The cell viability was evaluated by the WST-1 assay based changes in absorbance at 450 nm. Freshly isolated mouse HSCs or LX-2 cells were plated in 96-well plates at a density of 1.5×10^4 or 3×10^3 cells/well, respectively. The following day, cells were transfected with the miR-29b precursor or a negative

control as described above and were incubated for an additional 3 or 5 days before the assessment of cell viability. In another experiment, mouse HSCs that were transfected with the miR-29b precursor the day before were serum-starved overnight and then stimulated with PDGF-BB (10 ng/ml) (R&D Systems, Minneapolis, MO, USA). After incubation for 3 days, cell viability was assessed by the WST-1 assay.

2.7. Statistical analysis

Data presented as bar graphs are the means ± SD of at least three independent experiments. Statistical analysis was performed using the Student's *t*-test, and $P < 0.05$ was considered to be statistically significant.

3. Results and discussion

3.1. Expression of miR-29b in mouse HSCs during spontaneous activation

At 1 day of culture after isolation, mouse HSCs adhered to plastic plates and exhibited round cell bodies with numerous lipid droplets similar to those observed in lipocytes (Fig. 1A). Cell bodies then began to gradually spread and flatten, increasing in size, and losing lipid droplets, resulting in the activated myofibroblastic phenotype (Fig. 1A). In addition to the changes in cell appearance, mRNA expression levels of α-SMA, Col1a1, Col1a2, FN1, DDR2, ITGB1, and PDGFR-β significantly increased at Days 4 and 7 of culture as compared to Day 1 (Fig. 1B). Immunoblot analyses confirmed the increases of type I collagen, α-SMA, and PDGFR-β protein levels at Days 4 and 7 (Fig. 1C). These molecules have already been reported to be up-regulated in activated HSCs and involved in fibrosis [2]. Thus, the primary mouse HSCs used in this study were in an activated state. Although TGF-β1 is known as a key regulator of collagen production and fibrosis [13], its mRNA expression level in mouse HSCs remained unchanged due to an unknown reason in this study (Fig. 1B). In contrast, miR-29b expression in mouse HSCs was significantly decreased to 28% and 32% at Days 4 and 7, respectively, as compared to Day 1 (Fig. 1D). These findings raised the possibility that a reduction in miR-29b contributed to the up-regulation of the fibrosis-related genes listed above.

3.2. Effects of miR-29b overexpression on the activation of HSCs

To investigate this possibility, we next examined the effects of miR-29b overexpression on the activation of HSCs. Overexpression of miR-29b was achieved by the transient transfection of a synthesized miR-29b precursor, which was a double-strand RNA mimicking the endogenous miR-29b precursor. As shown in Fig. 2A, transfection of the miR-29b precursor markedly suppressed mRNA expression of Col1a1 and Col1a2 to 8% and 18%, respectively. Transfection significantly reduced mRNA expression of FN1 to 61% and also affected the expression of HSC activation-related molecules, such as α-SMA, DDR2, ITGB1, and PDGFR-β to 57%, 62%, 73%, and

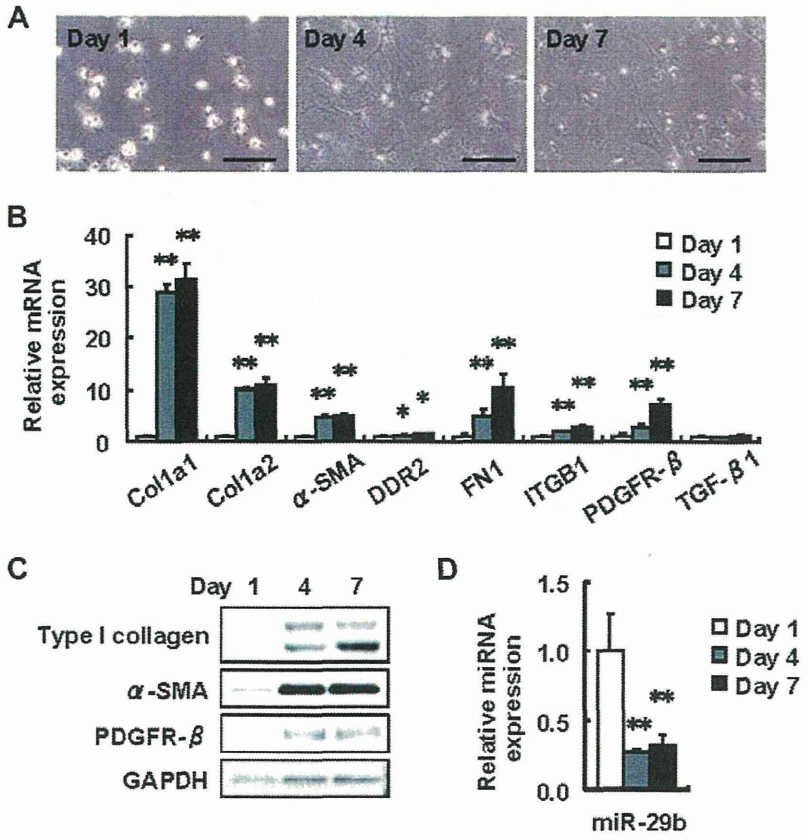

Fig. 1. Expression of miR-29b in mouse primary HSCs during culture. HSCs were isolated from mouse liver (Day 0) and cultured for the indicated periods. (A) Phase-contrast microscopy. Scale bar, 200 μm. (B) mRNA expression levels of Col1a1, Col1a2, α-SMA, DDR2, FN1, ITGB1, PDGFR-β and TGF-β1 were analyzed by real-time PCR. Results are expressed as relative expression against the expression on Day 1 of corresponding genes. $^{*}P < 0.05$, $^{**}P < 0.01$ compared with Day 1. (C) Protein expression levels of type I collagen, α-SMA and PDGFR-β were analyzed by Western blot. GAPDH served as an internal control. (D) miR-29b expression level was analyzed by real-time PCR. $^{*}P < 0.05$, $^{**}P < 0.01$ compared with Day 1.

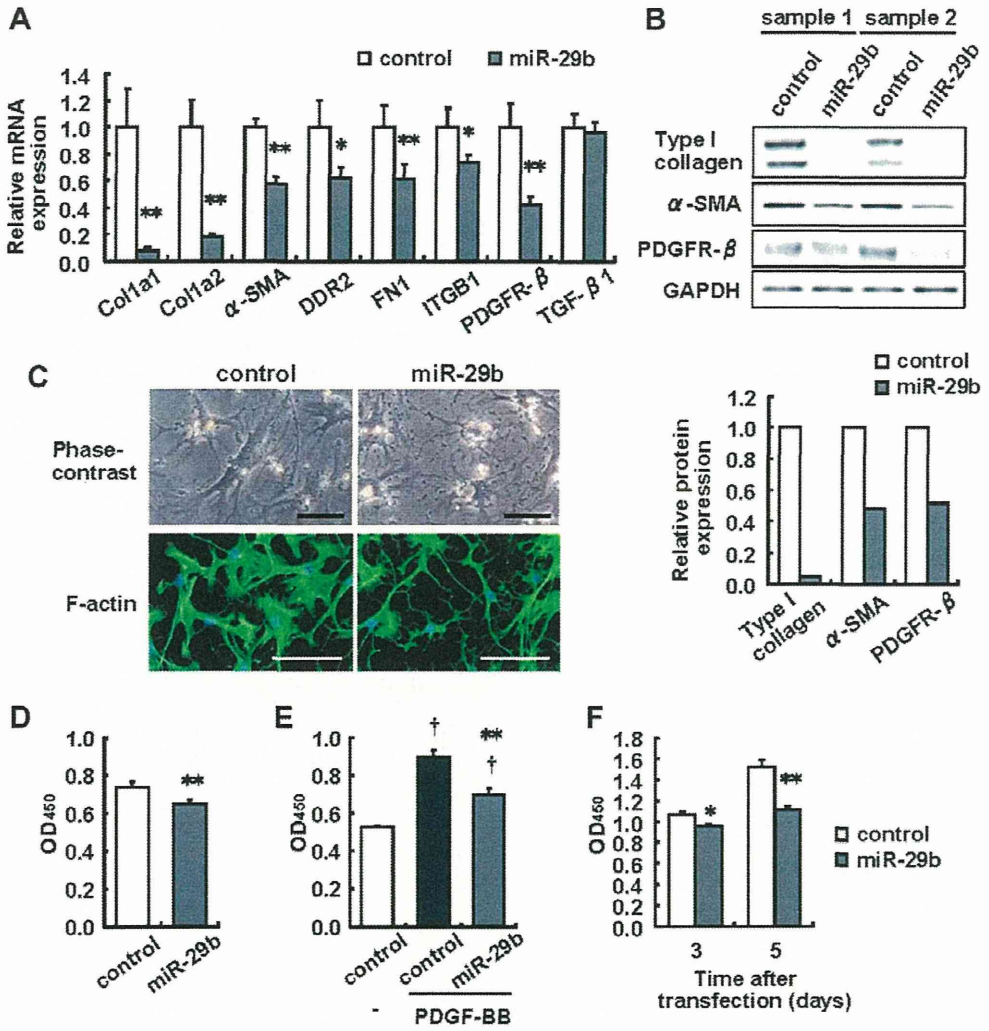

Fig. 2. Effects of miR-29b overexpression on the activation of HSCs. (A–D) Mouse HSCs were transfected with 10 nM miR-29b precursor or a negative control (control) on Day 1 and incubated for 3 days. (A) mRNA expression levels of Col1a1, Col1a2, α-SMA, DDR2, FN1, ITGB1, PDGFR-β and TGF-β1 were analyzed by real-time PCR. The results are expressed as relative expression against the expression of untreated control. $^{*}P < 0.05$, $^{**}P < 0.01$ compared with control. (B) Protein expression levels of type I collagen, α-SMA and PDGFR-β were analyzed by Western blot. GAPDH served as an internal control. The lower graph indicates the densitometric results of $n = 2$. (C) Phase-contrast microscopy (upper) and MFP488-phalloidin staining for F-actin (lower). Scale bar, 100 μm. (D) Cell viability was evaluated by WST-1 assay. $^{**}P < 0.01$ compared with control. (E) Mouse HSCs were transfected with miR-29b precursor or a negative control (control) on Day 1. Twenty-four hours later, cells were serum-starved overnight, stimulated with or without PDGF-BB (10 ng/ml) and incubated for an additional 3 days. In Day 6, cell viability was evaluated by WST-1 assay. $^{**}P < 0.01$ compared with control plus PDGF-BB. $^{\dagger}P < 0.05$ compared with control plus non-treat. (F) LX-2 cells were transfected with miR-29b precursor or a negative control (control) and incubated for the indicated periods. Cell viability was evaluated by WST-1 assay. $^{*}P < 0.05$, $^{**}P < 0.01$ compared with the control.

42%, respectively. The TGF-β1 mRNA level was unaffected. At the protein level, expression of type I collagen, α-SMA, and PDGFR-β was suppressed by the overexpression of the miR-29b precursor (Fig. 2B). Col1a1, Col1a2, ITGB1, and PDGFR-β are predicted targets of miR-29b according to the miRNA target prediction databases TargetScan (http://www.targetscan.org/), miRBase (http://www.mirbase.org/), and mircrorna.org (http://www.microrna.org). Therefore, the suppression of these proteins might be due to the direct interaction of miR-29b with the 3′UTR of their corresponding mRNAs. Although α-SMA, DDR2, and FN1 are not predicted targets of miR-29b, their mRNA levels were suppressed. Thus, this effect was thought to be a secondary action of miR-29b over-expression. That is, it is suggested that miR-29b can not only target Col1a1, Col1a2, ITGB1, and PDGFR-β, but can also suppress the activation of HSCs by regulating other unidentified mechanisms, resulting in the suppression of α-SMA, DDR2, and FN1. In support of these results, morphological transformation from the quiescent to the myofibroblastic cell shape, as shown in Fig. 1A, was impeded in miR-29b precursor-transfected cells (Fig. 2C); miR-29b precursor-transfected cells exhibited star-like morphology with small cell bodies and slender dendritic processes as compared to negative control-transfected cells at Day 4. Staining with MFP-phalloidin, which labels F-actin, also confirmed cytoskeletal changes in miR-29b precursor-transfected HSCs. Taken together; these results suggest that miR-29b is able to suppress HSC activation as well as ECM expression.

3.3. Effect of miR-29b overexpression on number of HSCs

Activated HSCs are known to acquire proliferation abilities [1,2]. We considered the possibility that miR-29b was able to regulate the number of HSCs. As shown by the WST-1 assay, when the miR-29b precursor was transfected into HSCs at Day 1, the cell number observed at Day 4 was significantly reduced to 88% of the negative control-transfected cells (Fig. 2D). Treatment of HSCs with 10 ng/mL PDGF-BB, a key mitogen for HSCs [14], significantly

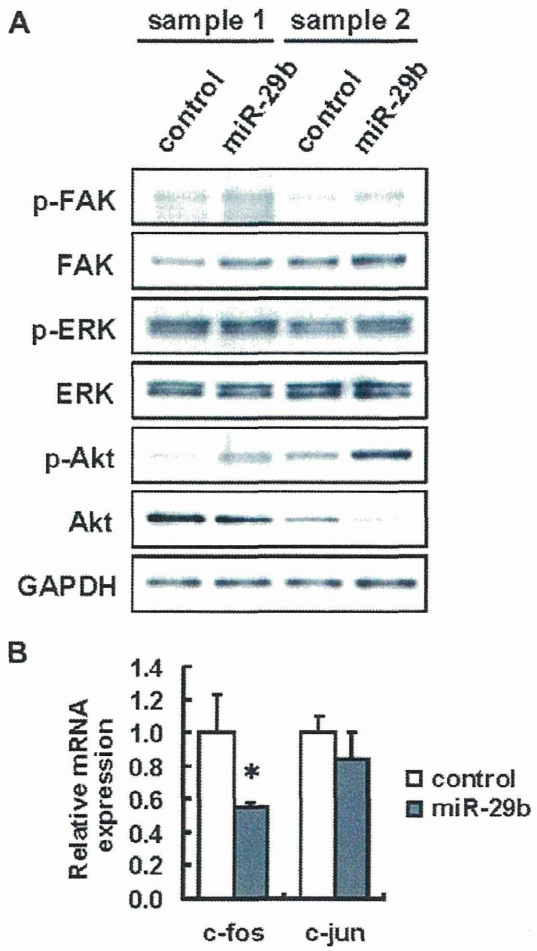

Fig. 3. Effects of miR-29b overexpression on the ECM- and growth factor-related signaling in mouse primary HSCs. Mouse HSCs were transfected with 10 nM miR-29b precursor or a negative control (control) on Day 1 and were incubated for 3 days. (A) Phosphorylation of FAK (Y397), ERK (T202/Y204) and Akt (S473) was analyzed by Western blot. (B) mRNA expression levels of c-fos and c-jun were analyzed by real-time PCR. The results are expressed as relative expression against the expression of control. $^{*}P < 0.05$ compared with control.

increased the cell number up to 1.7 times that of the non-treated cells (Fig. 2E), whereas overexpression of miR-29b inhibited this increase. Furthermore, in LX-2 cells, transfection of the miR-29b precursor decreased cell viability to 89% and 81% at 3 and 5 days following transfection, respectively (Fig. 2F). These results suggested that miR-29b is able to suppress the proliferation of HSCs and that down-regulation of miR-29b during HSC activation may contribute to their active proliferation.

3.4. Effects of miR-29b overexpression on the ECM- and growth factor-related signaling in primary mouse HSCs

The question of how miR-29b functions in blocking HSC activation was also examined. We showed that overexpression of miR-29b suppressed Col1a1, Col1a2, FN1, DDR2, ITGB1, and PDGFR-β expression (Fig. 2A and B). DDR2 is a receptor tyrosine kinase that is activated by the binding of collagen and was reported to be involved in the proliferation of HSCs and in the expression of matrix metalloproteinase-2 [15,16]. ITGB1 is a member of the integrin family and works as a FN or collagen receptor by forming a heterodimer with the integrin α subunit. ITGB1 is reported to be involved in the production of type I collagen and monocyte chemotactic protein-1 in HSCs [17,18]. PDGFR-β is a receptor of PDGF and is involved in the proliferation of activated HSCs [19,20]. Because it is known that intracellular signaling molecules such as FAK, ERK, and PI3K/Akt are key mediators for DDR2, ITGB1, and PDGFR-β [14,21–24], their down-regulation by miR-29b may affect downstream signaling, resulting in the inhibition of both activation and proliferation of HSCs. To verify this hypothesis, we investigated the effect of miR-29b overexpression on the activation of FAK, Akt, and ERK. Activation of these kinases was evaluated by immunoblot analyses to detect the phosphorylation of each protein. Unexpectedly, phosphorylation of FAK, ERK, and Akt was unaffected by miR-29b overexpression (Fig. 3A). Next, we also examined the mRNA expression of c-fos and c-jun, which form the transcription factor AP-1 complex and are located downstream of these signal kinases. Although transfection of the miR-29b precursor failed to alter c-jun expression, it significantly reduced c-fos mRNA expression to 55% (Fig. 3B). Because AP-1 is known to be one of the key transcription factors for the initiation of HSC activation [25,26], this fact indicates that effects of miR-29b may be partially mediated by c-fos down-regulation.

4. Conclusion

We confirmed that miR-29b expression decreased during HSC activation and found that overexpression of miR-29b is able to attenuate the activation and trans-differentiation of HSCs, although the precise molecular mechanism for this effect remains unknown. Changes in miR-29b expression seem to profoundly affect the activation of HSCs.

Conflict of interest

The authors have no conflict of interest to declare.

Acknowledgment

This work was supported by a grant from the Ministry of Health, Labor and Welfare of Japan to N. Kawada (2008–2010).

References

[1] R. Bataller, D.A. Brenner, Hepatic stellate cells as a target for the treatment of liver fibrosis, Semin. Liver Dis. 21 (2001) 437–451.
[2] S.L. Friedman, Molecular regulation of hepatic fibrosis an integrated cellular response to tissue injury, J. Biol. Chem. 275 (2000) 2247–2250.
[3] D.P. Bartel, MicroRNAs: genomics, biogenesis, mechanism, and function, Cell 116 (2004) 281–297.
[4] C.J. Guo, Q. Pan, B. Jiang, G.Y. Chen, D.G. Li, Effects of upregulated expression of microRNA-16 on biological properties of culture-activated hepatic stellate cells, Apoptosis 14 (2009) 1331–1340.
[5] C.J. Guo, Q. Pan, D.G. Li, H. Sun, B.W. Liu, miR-15b and miR-16 are implicated in activation of the rat hepatic stellate cell: an essential role for apoptosis, J. Hepatol. 50 (2009) 766–778.
[6] J.L. Ji, J.S. Zhang, G.C. Huang, J. Qian, X.Q. Wang, S. Mei, Over-expressed microRNA-27a and 27b influence fat accumulation and cell proliferation during rat hepatic stellate cell activation, FEBS Lett. 583 (2009) 759–766.
[7] S.K. Venugopal, J. Jiang, T.H. Kim, Y. Li, S.S. Wang, N.J. Torok, J. Wu, M.A. Zern, Liver fibrosis causes downregulation of miRNA-150 and miRNA-194 in hepatic stellate cells, and their overexpression causes decreased stellate cell activation, Am. J. Physiol. Gastrointest. Liver Physiol. 298 (2010) G101–G106.
[8] Y. Sekiya, T. Ogawa, M. Iizuka, K. Yoshizato, K. Ikeda, N. Kawada, Down-regulation of cyclin E1 expression by microRNA-195 accounts for interferon-β-induced inhibition of hepatic stellate cell proliferation, J. Cell. Physiol. 2010, doi:10.1002/jcp22598.
[9] T. Ogawa, M. Iizuka, Y. Sekiya, K. Yoshizato, K. Ikeda, N. Kawada, Suppression of type I collagen production by microRNA-29b in cultured human stellate cells, Biochem. Biophys. Res. Commun. 391 (2010) 316–321.
[10] C. Roderburg, G.W. Urban, K. Bettermann, M. Vucur, H. Zimmermann, S. Schmidt, J. Janssen, C. Koppe, P. Knolle, M. Castoldi, F. Tacke, C. Trautwein, T. Luedde, Micro-RNA profiling reveals a role for miR-29 in human and murine liver fibrosis, Hepatology 53 (2011) 209–218.

[11] N. Uyama, L. Zhao, E. Van Rossen, Y. Hirako, H. Reynaert, D.H. Adams, Z. Xue, Z. Li, R. Robson, M. Pekny, A. Geerts, Hepatic stellate cells express synemin, a protein bridging intermediate filaments to focal adhesions, Gut 55 (2006) 1276–1289.

[12] L. Xu, A.Y. Hui, E. Albanis, M.J. Arthur, S.M. O'Byrne, W.S. Blaner, P. Mukherjee, S.L. Friedman, F.J. Eng, Human hepatic stellate cell lines, LX-1 and LX-2: new tools for analysis of hepatic fibrosis, Gut 54 (2005) 142–151.

[13] D.M. Bissell, D. Roulot, J. George, Transforming growth factor beta and the liver, Hepatology 34 (2001) 859–867.

[14] F. Marra, M. Pinzani, R. Defranco, G. Laffi, P. Gentilini, Involvement of phosphatidylinositol 3-kinase in the activation of extracellular signal-regulated kinase by PDGF in hepatic stellate cells, FEBS Lett. 376 (1995) 141–145.

[15] E. Olaso, K. Ikeda, F.J. Eng, L.M. Xu, L.H. Wang, H.C. Lin, S.L. Friedman, DDR2 receptor promotes MMP-2-mediated proliferation and invasion by hepatic stellate cells, J. Clin. Invest. 108 (2001) 1369–1378.

[16] E. Olaso, J.P. Labrador, L.H. Wang, K. Ikeda, F.J. Eng, R. Klein, D.H. Lovett, H.C. Lin, S.L. Friedman, Discoidin domain receptor 2 regulates fibroblast proliferation and migration through the extracellular matrix in association with transcriptional activation of matrix metalloproteinase-2, J. Biol. Chem. 277 (2002) 3606–3613.

[17] F. Marra, S. Pastacaldi, R.G. Romanelli, M. Pinzani, P. Ticali, V. Carloni, G. Laffi, P. Gentilini, Integrin-mediated stimulation of monocyte chemotactic protein-1 expression, FEBS Lett. 414 (1997) 221–225.

[18] D.R. Wang, M. Sato, L.N. Li, M. Miura, N. Kojima, H. Senoo, Stimulation of pro-MMP-2 production and activation by native form of extracellular type I collagen in cultured hepatic stellate cells, Cell Struct. Funct. 28 (2003) 505–513.

[19] E. Borkham-Kamphorst, J. Herrmann, D. Stoll, J. Treptau, A.M. Gressner, R. Weiskirchen, Dominant-negative soluble PDGF-beta receptor inhibits hepatic stellate cell activation and attenuates liver fibrosis, Lab. Invest. 84 (2004) 766–777.

[20] C.G. Lechuga, Z.H. Hernandez-Nazara, E. Hernandez, M. Bustamante, G. Desierto, A. Cotty, N. Dharker, M. Choe, M. Rojkind, PI3K is involved in PDGF-beta receptor upregulation post-PDGF-BB treatment in mouse HSC, Am, J. Physiol. Gastrointest. Liver Physiol. 291 (2006) G1051–G1061.

[21] V. Carloni, R.G. Romanelli, M. Pinzani, G. Laffi, P. Gentilini, Focal adhesion kinase and phospholipase C gamma involvement in adhesion and migration of human hepatic stellate cells, Gastroenterology 112 (1997) 522–531.

[22] C. Rodriguez-Juan, P. de la Torre, I. Garcia-Ruiz, T. Diaz-Sanjuan, T. Munoz-Yague, E. Gomez-Izquierdo, P. Solis-Munoz, J.A. Solis-Herruzo, Fibronectin increases survival of rat hepatic stellate cells – a novel profibrogenic mechanism of fibronectin, Cell. Physiol. Biochem. 24 (2009) 271–282.

[23] H.J. Wu, Z.Q. Zhang, B. Yu, S. Liu, K.R. Qin, L.A. Zhu, Pressure activates Src-dependent FAK–Akt and ERK1/2 signaling pathways in rat hepatic stellate cells, Cell. Physiol. Biochem. 26 (2010) 273–280.

[24] K. Ikeda, L.H. Wang, R. Torres, H. Zhao, E. Olaso, F.J. Eng, P. Labrador, R. Klein, D. Lovett, G.D. Yancopoulos, S.L. Friedman, H.C. Lin, Discoidin domain receptor 2 interacts with Src and Shc following its activation by type I collagen, J. Biol. Chem. 277 (2002) 19206–19212.

[25] R. Gao, D.K. Ball, B. Perbal, D.R. Brigstock, Connective tissue growth factor induces c-fos gene activation and cell proliferation through p44/42 MAP kinase in primary rat hepatic stellate cells, J. Hepatol. 40 (2004) 431–438.

[26] J.E. Poulos, J.D. Weber, J.M. Bellezzo, A.M.D. Bisceglie, R.S. Britton, B.R. Bacon, J.J. Baldassare, Fibronectin and cytokines increase JNK, ERK, AP-1 activity, and transin gene expression in rat hepatic stellate cells, Am. J. Physiol. 273 (1997) G804–G811.

Journal of Cellular Physiology

Down-Regulation of Cyclin E1 Expression by MicroRNA-195 Accounts for Interferon-β-Induced Inhibition of Hepatic Stellate Cell Proliferation

YUMIKO SEKIYA,[1,2] TOMOHIRO OGAWA,[1,2] MASASHI IIZUKA,[1,2] KATSUTOSHI YOSHIZATO,[1,2,3] KAZUO IKEDA,[4] AND NORIFUMI KAWADA[1,2]*

[1]*Department of Hepatology, Graduate School of Medicine, Osaka City University, Osaka, Japan*

[2]*Liver Research Center, Graduate School of Medicine, Osaka City University, Osaka, Japan*

[3]*PhoenixBio Co. Ltd., Hiroshima, Japan*

[4]*Department of Anatomy and Cell Biology, Graduate School of Medical Sciences, Nagoya City University, Aichi, Japan*

Recent studies have suggested that interferons (IFNs) have an antifibrotic effect in the liver independent of their antiviral effect although its detailed mechanism remains largely unknown. Some microRNAs have been reported to regulate pathophysiological activities of hepatic stellate cells (HSCs). We performed analyses of the antiproliferative effects of IFNs in HSCs with special regard to microRNA-195 (miR-195). We found that miR-195 was prominently down-regulated in the proliferative phase of primary-cultured mouse HSCs. Supporting this fact, IFN-β induced miR-195 expression and inhibited the cell proliferation by delaying their G1 to S phase cell cycle progression in human HSC line LX-2. IFN-β down-regulated cyclin E1 and up-regulated p21 mRNA levels in LX-2 cells. Luciferase reporter assay revealed the direct interaction of miR-195 with the cyclin E1 3′UTR. Overexpression of miR-195 lowered cyclin E1 mRNA and protein expression levels, increased p21 mRNA and protein expression levels, and inhibited cell proliferation in LX-2 cells. Moreover miR-195 inhibition restored cyclin E1 levels that were down-regulated by IFN-β. In conclusion, IFN-β inhibited the proliferation of LX-2 cells by delaying cell cycle progression in G1 to S phase, partially through the down-regulation of cyclin E1 and up-regulation of p21. IFN-induced miR-195 was involved in these processes. These observations reveal a new mechanistic aspect of the antifibrotic effect of IFNs in the liver.

J. Cell. Physiol. 226: 2535–2542, 2011.

Hepatic fibrosis is characterized by excessive accumulation of extracellular matrices (ECM) and is a common feature of chronic liver diseases. Hepatic stellate cells (HSCs) are considered to play multiple roles in the fibrotic process. HSCs maintain a quiescent phenotype and store vitamin A under physiological conditions. When liver injury occurs, they become activated and trans-differentiate into myofibroblastic cells, whose characteristics include the proliferation, loss of vitamin A droplets, expression of α-smooth muscle actin (α-SMA), secretion of profibrogenic mediators and ECM (Friedman, 2000; Bataller and Brenner, 2001). Therefore, controlling the population and activation of HSCs should be a potential therapeutic target against liver fibrosis.

Interferons (IFNs) are cytokines with antiviral, immunomodulatory, and cell growth inhibitory effects. IFN-α and -β are classified as type I IFNs (Pestka et al., 1987; Uze et al., 2007), which are generally applied for the therapy of eradication of hepatitis B and C viruses. Studies using rodent models and cultured HSCs have also suggested that IFNs have a direct antifibrotic potential independently of their antivirus activity (Mallat et al., 1995; Fort et al., 1998; Shen et al., 2002; Inagaki et al., 2003; Chang et al., 2005; Tanabe et al., 2007; Ogawa et al., 2009), although the detailed molecular mechanisms of these effects of IFNs remain to be clarified.

Recently, microRNAs (miRNAs), which are endogenous small non-coding RNA, have become a focus of interest as post-transcriptional regulators of gene expression through interaction with the 3′ untranslated region (3′UTR) of target mRNAs (Bartel, 2004). miRNAs are known to participate in cell proliferation, development, differentiation, and metabolism (Bartel, 2004). Moreover, it has been reported that expression of miRNAs could alter hepatic pathophysiology; microRNA-122 (miR-122) is involved in the IFN-β-related defense system against viral hepatitis C (Pedersen et al., 2007), and miR-26 is associated with survival and response to adjuvant IFN-α therapy in patients with hepatocellular carcinoma (HCC) (Ji et al., 2009a). Regarding HSCs, miR-15b and miR-16 are down-regulated upon HSC's activation, and their overexpression induces apoptosis and a delay in the cell cycle (Guo et al., 2009a,b). Knockdown of miR-27a and miR-27b in activated HSCs allowed a switch to a more quiescent phenotype and decreased cell proliferation (Ji et al., 2009b). miR-150 and miR-194 suppress proliferation, activation, and ECM production of HSCs (Venugopal et al., 2010). Recently, we showed that miR-29b was induced by IFN and suppressed type I collagen production in LX-2 cells (Ogawa et al., 2010).

In the present study, we measured the levels of miR-195 in primary-cultured mouse HSCs and found that its expression was markedly reduced in their activation phase, suggesting the regulatory role of miR-195 in the activation/deactivation process of

Contract grant sponsor: The Ministry of Health, Labour and Welfare of Japan;
Contract grant number: 2008-KAKEN-IPPAN-003.

*Correspondence to: Norifumi Kawada, Department of Hepatology, Graduate School of Medicine, Osaka City University, 1-4-3, Asahimachi, Abeno, Osaka 545-8585, Japan.
E-mail: kawadanori@med.osaka-cu.ac.jp

Received 6 September 2010; Accepted 3 December 2010

Published online in Wiley Online Library (wileyonlinelibrary.com), 29 December 2010.
DOI: 10.1002/jcp.22598

TABLE 1. Sequences of primers used in real-time PCR analyses and 3′UTR cloning for luciferase reporter assay

Gene	Accession no.	Sequence
Real-time PCR		
CDK2	NM_001798	Forward: 5′-CTCCACCGAGACCTTAAACCTCAG-3′ Reverse: 5′-TCGGTACCACAGGGTCACCA-3′
CDK4	NM_000075	Forward: 5′-GATAGATGCTGACCCATACCTCAAG-3′ Reverse: 5′-ATGCTGTGGTGCTTTGAGGTAG-3
CDK6	NM_001259	Forward: 5′-ATATCTGCCTACAGTGCCCTGTCTC-3′ Reverse: 5′-GTGGGAATCCAGGTTTTCTTTGCAC-3′
Cyclin E1	NM_001238	Forward: 5′-GCAGTATCCCCAGCAAATC-3′ Reverse: 5′-TCAAGGCAGTCAACATCCA-3′
Cyclin D1	NM_053056	Forward: 5′-GCTGTGCATCTACACCGACAACTC-3′ Reverse: 5′-AGGTTCCACTTGAGCTTGTTCACC-3′
E2F3	NM_001949	Forward: 5′-CCAACTCAGGACATAGCGATTGCTC-3′ Reverse: 5′-AGGAATTTGGTCCTCAGTCTGCTGT-3′
GAPDH	NM_002046	Forward: 5′-GCACCGTCAAGGCTGAGAAC-3′ Reverse: 5′-TGGTGAAGACGCCAGTGGA-3′
p21	NM_000389	Forward: 5′-AGCAGAGGAAGACCATGTGGA-3′ Reverse: 5′-GGAGTGGTAGAAATCTGTCATGCT-3′
p27	NM_004064	Forward: 5′-AGCTTGCCCGAGTTCTACTACAG-3′ Reverse: 5′-ACCAAATGCGTGTCCTCAGAGT-3′
3′UTR cloning		
Cyclin E1	NM_001238	Forward: 5′-TTCTCGAGATCCTTCTCCACCAAAGACAGTT-3′ Reverse: 5′-TTTCTAGAGAATGGATAGATATAGCAGCACTTACA-3′

The forward and reverse primers for 3′UTR cloning carried the *Xho*I and *Xba*I sites at their 5′-ends, respectively.

HSCs. Because miR-195 is categorized into the same family as miR-15b and miR-16 and has been reported to regulate cell cycle by targeting E2F3, CDK6, and cyclin D1 (Xu et al., 2009), we suspect the involvement of miR-195 in the proliferation of HSC and in type I IFN, in particular IFN-β, -induced inhibition of their growth.

Materials and Methods

Materials

Human HSC line LX-2 was donated by Dr. Scott L. Friedman (Mount Sinai School of Medicine, New York, NY) (Xu et al., 2005). Necessary reagents and materials were obtained from the

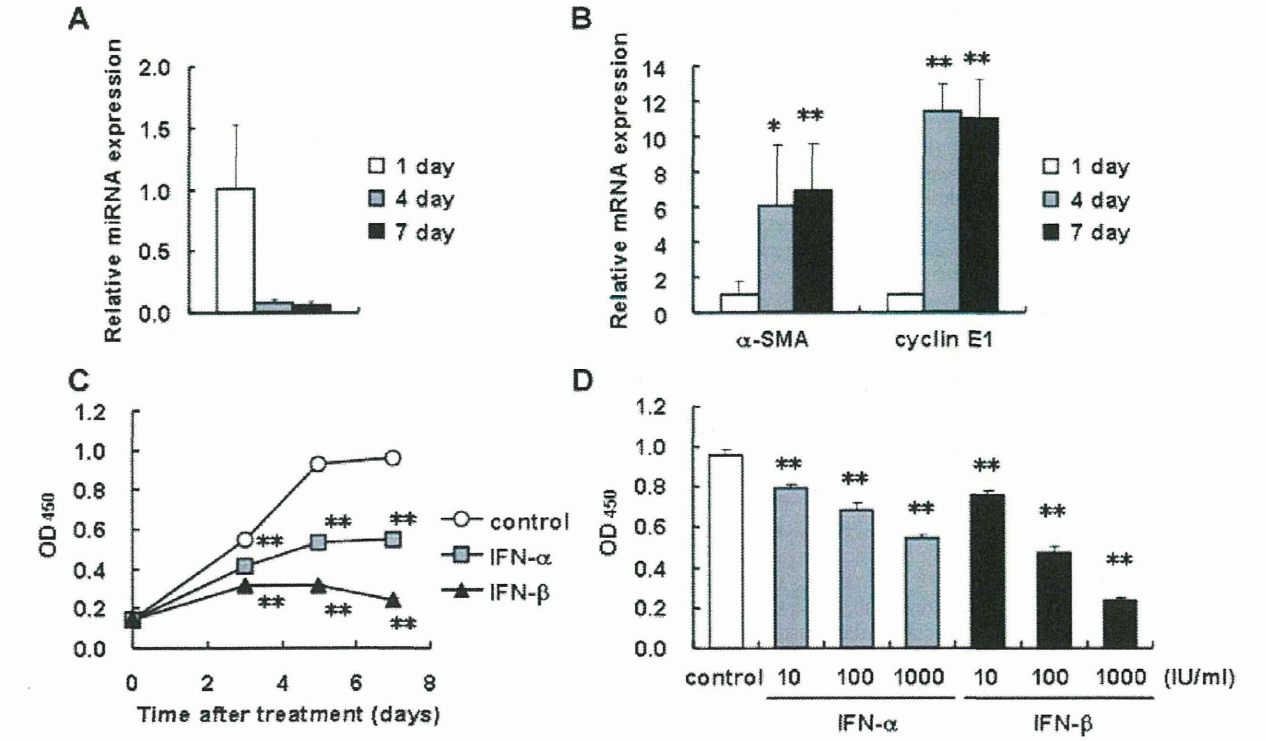

Fig. 1. Expression of miR-195 in mouse HSCs during primary culture and growth inhibitory effect of IFN-α and -β on human stellate cells. A,B: Isolated mouse HSCs were cultured for the indicated periods. The expression levels of miR-195 (A), and α-SMA and cyclin E1 mRNA (B) were measured by real-time PCR. *$P < 0.05$, **$P < 0.01$ compared with 1 day. C,D: LX-2 cells were incubated with IFN-α or -β (1,000 IU/ml) for 3–7 days (C), or with IFN-α or -β at the concentration of 10–1,000 IU/ml for 7 days (D). Control indicates non-treated cells. The proportion of viable cells was determined using a WST-1 assay. **$P < 0.01$ compared with control.

following sources: Dulbecco's modified Eagle's medium (DMEM) from Sigma Chemical Co. (St. Louis, MO); fetal bovine serum (FBS) from Invitrogen (Carlsbad, CA); human natural IFN-α and -β from Otsuka Pharmaceutical Co. (Tokushima, Japan) and Toray Industries, Inc. (Tokyo, Japan), respectively; precursor and inhibitor of miR-195, and the corresponding negative controls from Ambion (Austin, TX); mouse monoclonal antibody against cyclin E1, cyclin D1 and p21, and glyceraldehyde-3-phosphate dehydrogenase (GAPDH) from MBL (Nagoya, Japan), Cell Signaling Technology, Inc. (Beverly, MA), and Chemicon International, Inc. (Temecula, CA), respectively; rabbit polyclonal antibodies against cyclin-dependent kinase (CDK) 6 and E2F3 from Santa Cruz Biotechnology, Inc. (Santa Cruz, CA); goat polyclonal antibody against CDK4 from Santa Cruz Biotechnology, Inc.; enhanced Chemiluminescence plus detection reagent from GE Healthcare (Buckinghamshire, UK); Immobilon P membranes from Millipore Corp. (Bedford, MA); reagents for cDNA synthesis and real-time PCR from Toyobo (Osaka, Japan); a cell counting kit from Dojindo Laboratories (Kumamoto, Japan); and all other reagents from Sigma Chemical Co. or Wako Pure Chemical Co. (Osaka, Japan).

Cells

LX-2 cells were maintained in DMEM supplemented with 10% FBS (DMEM/FBS) and were plated at a density of 0.7–1.5 × 10^4 cells/cm^2 24 h prior to biological assay. Biological assays were done in DMEM/FBS unless stated otherwise. Mouse primary HSCs were isolated from male C57BL/6 mice by the pronase-collagenase digestion method as described previously (Uyama et al., 2006) and were cultured in DMEM/FBS.

Transient transfection of miRNA precursors and inhibitors

Precursor of miR-195, which was a double-strand RNA mimicking endogenous miR-195 precursor, and the negative control with a scrambled sequence were transfected into LX-2 cells using Lipofectamine 2000 (Invitrogen) at a final concentration of 50 nM in accordance with the manufacturer's instructions. Briefly, miRNA precursor and Lipofectamine 2000 were mixed at a ratio of 25 (pmol):1 (μl) in Opti-MEM I Reduced Medium (Invitrogen), incubated for 20 min at room temperature, and were then added to the cultures. After 24 h, the culture medium was replaced with fresh medium. Inhibitor of miR-195, which was designed to bind to endogenous miR-195 and inhibit its activity, and the negative control with a scrambled sequence were transfected similarly. After 6 h, the culture medium was changed and IFN-β was added successively.

Cell proliferation assay

LX-2 cells were plated at a density of 2 × 10^3 cells/well in 96-well plates 24 h prior to experiments. The culture medium was replaced by fresh medium containing different concentrations of IFNs at days 0 and 3. After 3, 5, and 7 days of treatment, cell proliferation was measured by WST-1 assay. In another experiment, the cells

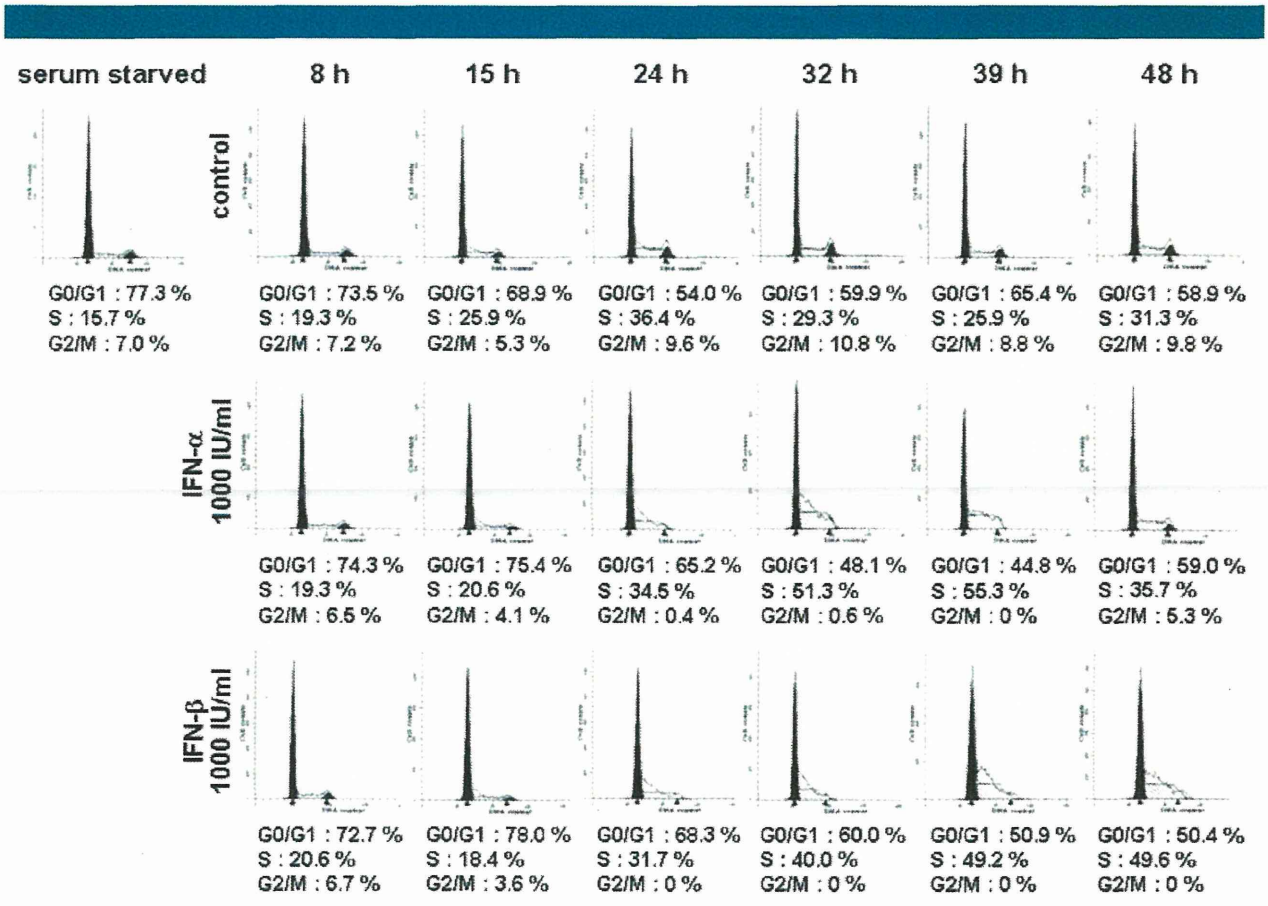

Fig. 2. Effect of IFN-α and -β on cell cycle distribution in human stellate cells. LX-2 cells synchronized in G0/G1 phase were then incubated with IFN-α or -β (1,000 IU/ml) in DMEM/FBS for the indicated periods. Control indicates non-treated cells. The cell cycle was analyzed by flow cytometry. The white, black, and shaded region indicates the histogram measured by flow cytometry, G0/G1 phase (left) or G2/M phase (right), and S phase, respectively, as analyzed by ModFIT LT software.

were plated at a density of 3×10^3 cells/well in 96-well plate for 24 h prior and were then transfected with the miR-195 precursor as described above. After 24 h, the medium was changed and the culture was continued for an additional 1–3 days before the measurement of cell proliferation.

Cell cycle analysis

Cells were serum starved for 24 h and then the medium was replaced with IFN-containing DMEM/FBS. At the indicated time points after treatment, the cells were harvested by trypsinization, washed in phosphate-buffered saline (PBS), and fixed in ice-cold 70% ethanol. The cells were washed in PBS and resuspended in PBS containing 500 μg/ml RNase A and incubated for 20 min. Cellular DNA was stained with propidium iodide at a final concentration of 25 μg/ml for 20 min. The cells were analyzed using a FACSCalibur HG flow cytometer (Becton Dickinson, Franklin Lakes, NJ). A total of 20,000 events were counted for each sample. Data were analyzed using ModFIT LT software (Verity Software House, Topsham, ME).

Quantitative real-time PCR

Quantitative real-time PCR was performed according to the method described elsewhere with use of a set of gene-specific oligonucleotide primers (Table 1) using an Applied Biosystems Prism 7500 (Applied Biosystems, Foster City, CA) (Ogawa et al., 2010). To detect miR-195 expression, the reverse transcription reaction was performed using a TaqMan microRNA Assay (Applied Biosystems) in accordance with the manufacturer's instructions. The expression level of GAPDH was used to normalize the relative abundance of mRNAs and miR-195.

Immunoblotting

Cells were lysed in RIPA buffer [50 mM Tris/HCl, pH 7.5, 150 mM NaCl, 1% NP-40, 0.5% sodium deoxycholate, 0.1% sodium dodecyl sulfate (SDS)] containing Protease Inhibitor Cocktail, Phosphatase Inhibitors Cocktail 1, and Phosphatase Inhibitor Cocktail 2 (Sigma). Proteins (20 μg) were electrophoresed in a 10% SDS–polyacrylamide gel and then transferred onto Immobilon P membranes (Ogawa et al., 2010). Immunoreactive bands were visualized by the enhanced chemiluminescence system using a Fujifilm Image Reader LAS-3000 (Fuji Medical Systems, Stamford, CT).

Luciferase reporter assay

Interaction of miR-195 to the 3′UTR of the cyclin E1 gene was tested according to the reported method (Ogawa et al., 2010). The 3′UTR of the cyclin E1 gene containing putative miR-195 target regions was obtained by PCR using cDNA derived from LX-2 and a primer set listed in Table 1. The obtained DNA fragments (497 bp) were inserted into a pmirGLO Vector (Promega, San Luis Obispo,

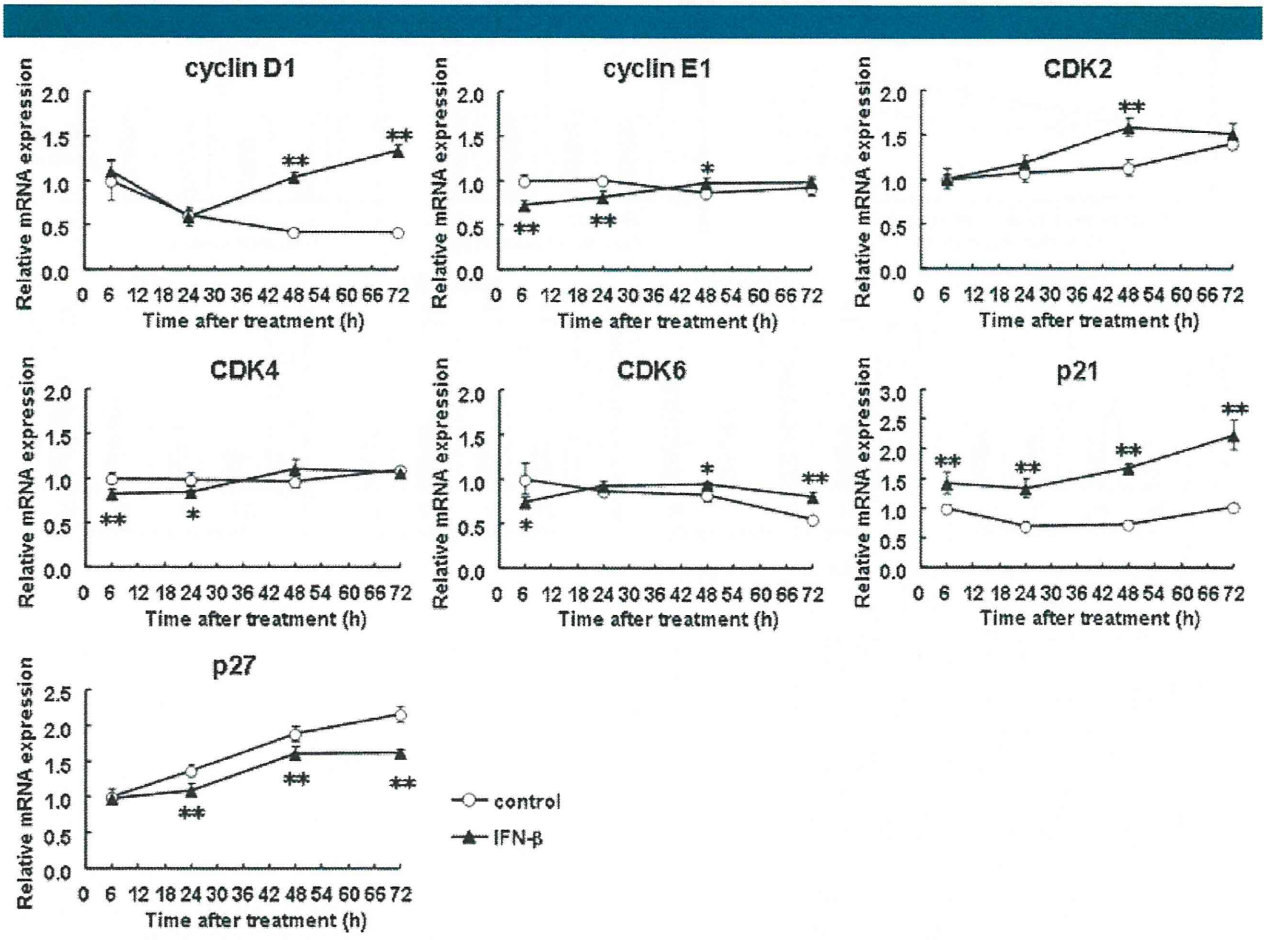

Fig. 3. Expression of cell cycle-related genes in stellate cells. LX-2 cells were incubated with IFN-β (1,000 IU/ml) for up to 72 h for determining the expression levels of mRNAs of cyclin D1, cyclin E1, CDK2, CDK4, CDK6, p21, and p27. Control indicates non-treated cells. *$P < 0.05$, **$P < 0.01$ compared with control.

CA). LX-2 cells, plated in 96-well plates at a density of 2×10^4 cells/well 24 h prior to experiment, were transfected with 200 ng of reporter plasmid and miRNA precursor using Lipofectamine 2000. After 24 h, the medium was changed to 20 μl of PBS. The Dual-Glo Luciferase Assay System (Promega) was used to analyze luciferase expression in accordance with the manufacturer's protocol. Firefly luciferase activity was normalized to *Renilla* luciferase activity to adjust for variations in transfection efficiency among experiments.

Statistical analysis

Data presented as graphs are the means ± SD of at least three independent experiments. Statistical analysis was performed using Student's *t*-test. $P < 0.05$ was considered significant.

Results

Reduction of miR-195 expression during activation of primary-cultured HSCs

It has been known that, when maintained in a plastic culture plate, freshly isolated primary-cultured HSCs undergo spontaneous activation and transformation into myofibroblastic cells that express α-SMA and produce fibrogenic mediators, such as type I collagen and transforming growth factor-β. In our preliminary experiments using primary-cultured mouse HSCs, we noticed that the cells drastically decreased the expression of miR-195 when they underwent spontaneous activation (unpublished observation). The present study confirmed this notion as shown in Figure 1A. miR-195 expression level certainly decreased in activation process of primary-cultured mouse HSCs. In contrast, the expression levels of α-SMA and cyclin E1 mRNA increased (Fig. 1B). Accordingly, we considered that miR-195 plays a role as an antiproliferative and antiactivating miRNA in HSCs. As a matter of fact, there was a study showing that miR-16 family including miR-195 inhibits proliferation of lung cancer cells by silencing cyclins D1 and E1, and CDK6 (Liu et al., 2008). The result indicated by Figure 1 and the cited study together drove us to explore the IFN's antiproliferative action on HSCs (Mallat et al., 1995; Shen et al., 2002), focusing on miR-195 and cell cycle-related genes.

Effects of IFN-α and -β on proliferation of HSCs

First, we investigated the effects of type I IFNs on the proliferation of LX-2 cells using a WST-1 assay. LX-2 cells in control culture continued to grow during the experimental

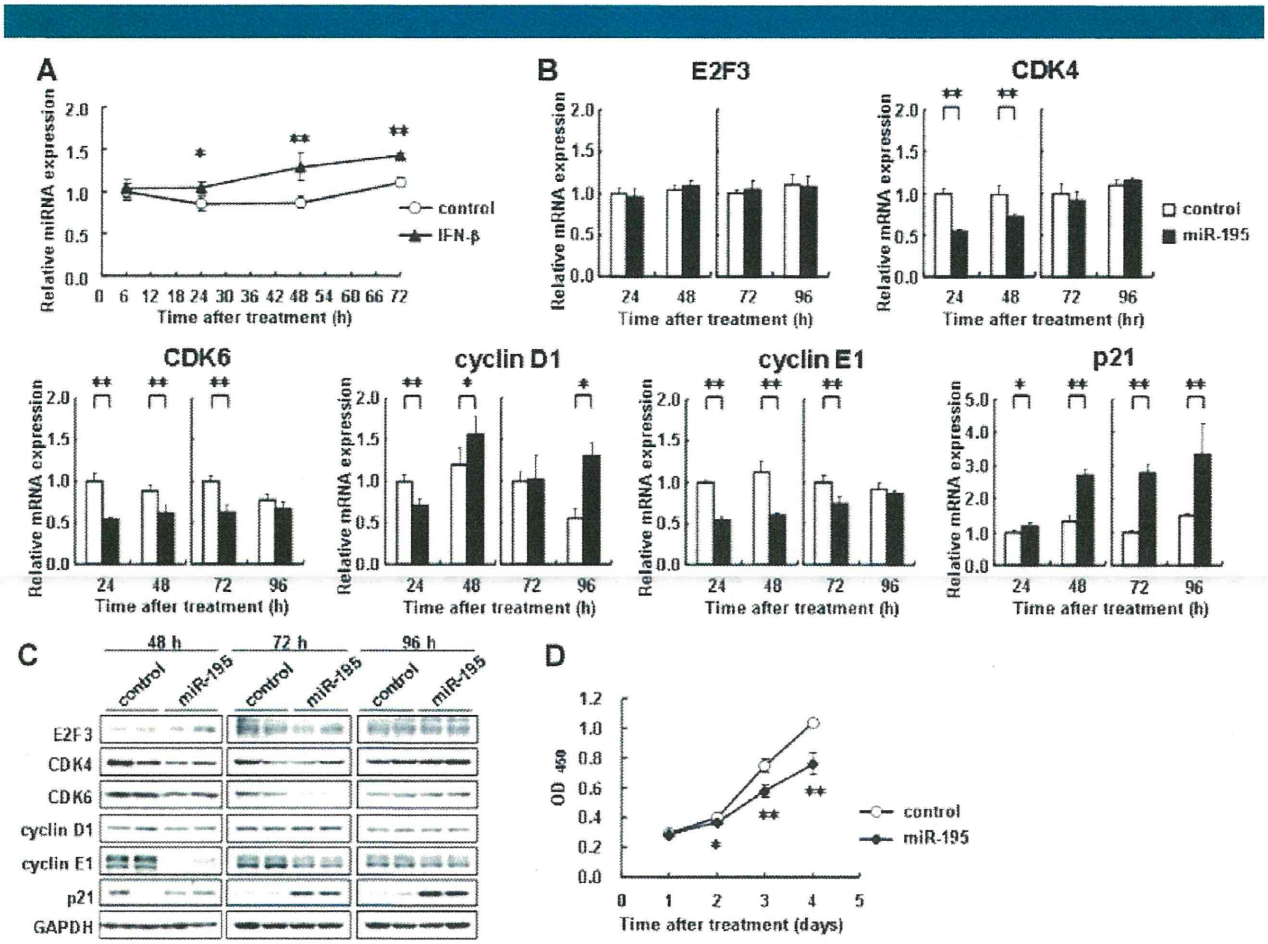

Fig. 4. Regulation of expression of cell cycle regulators by miR-195. A: LX-2 cells were incubated with IFN-β (1,000 IU/ml) for up to 72 h for determining the expression levels of miR-195. Control indicates non-treated cells. *$P < 0.05$, **$P < 0.01$ compared with control. B–D: LX-2 cells were transfected with 50 nM miR-195 precursor or a negative control (control). B: mRNA expression levels of E2F3, CDK4, CDK6, cyclin D1, cyclin E1, and p21 measured at 24, 48, 72, and 96 h post-transfection. C: Protein expression of E2F3, CDK4, CDK6, cyclin D1, cyclin E1, and p21 examined at 48, 72, and 96 h post-transfection. D: Growth of LX-2 cells transfected with 50 nM miR-195 precursor or a negative control (control) was measured using a WST-1 assay. *$P < 0.05$, **$P < 0.01$ compared with control.